Available online at www.sciencedirect.com

ScienceDirect

Physics Procedia 59 (2014) 42 – 47

Physics Procedia

GAMMA-2 Scientific Workshop on the Emission of Prompt Gamma-Rays in Fission and Related Topics

Photofission fragment characteristics of ^{234,238}U and ^{232}Th in the barrier region

A. Göök[a,b,*], M. Freudenberger[a], J. Enders[a], C. Eckardt[a], A. Oberstedt[c], S. Oberstedt[b]

[a] *Institut für Kernphysik, Technische Universität Darmstadt, Schlossgartenstraße 9, 64293 Darmstadt, Germany*
[b] *European Commission, DG Joint Research Centre (IRMM), 2440 Geel, Belgium*
[c] *Fundamental Fysik, Chalmers Tekniska Högskola, 41296 Göteborg, Sweden*

Abstract

The bremstrahlung induced fission of ^{234,238}U and ^{232}Th has been studied at the superconducting Darmstadt linear accelerator (S-DALINAC) in the excitation energy region close to the fission barrier. In this contribution results on the fission fragment mass, total kinetic energy (TKE) and angular distributions will be presented. Fission fragment mass and TKE distributions from ^{234}U were studied for the first time in this energy region. The results have been analyzed in terms of fission modes and a dominant yield of the mass asymmetric standard-2 mode was found in all studied nuclei. No strong dependence of the fission mode weights on the excitation energy of the compound nucleus were found. Correlations between mass, TKE and angular distributions have been investigated in ^{234}U and ^{232}Th. A correlation in form of an increased anisotropy for far-asymmetric masses and low TKE were found in both fissioning systems. A possible interpretation of this correlation in terms of fission modes is discussed.

Selection and peer-review under responsibility of Guest Editor: Mr. Stephan Oberstedt - stephan.oberstedt@ec.europa.eu

Keywords: Photofission, Mass, TKE, Angular distribution;

1. Introduction

Near-barrier fission proceeds through a few low-lying collective excitations, the so-called transition states (Bohr, 1956). The absorption of real photons takes place mainly as an E1 excitation offering low-energy photofission of even-even nuclei the advantage of spin selectivity. The sequence of transition states on top of the fission barrier is sensitive to the barrier structure, and is reflected in the angular distribution of fission fragments. A long standing question concerns the possibility of correlations between fission fragment mass and angular distribution. If there exists different paths through the landscape of the fission barrier, leading to different mass splits, one may expect differences in the available transition states for these paths and thereby a correlation between fission-fragment mass and angular distributions. Such correlations have been found to exist in photofission (Wilke et al., 1988; Steiper et al., 1993). We have performed systematic studies of fission fragment characteristics, including mass and angular

* Corresponding author. Tel.: +32 (0)14 57 3038.
E-mail address: alf.gook@ec.europa.eu

Selection and peer-review under responsibility of Guest Editor: Mr. Stephan Oberstedt - stephan.oberstedt@ec.europa.eu
doi:10.1016/j.phpro.2014.10.007

distribution correlations in the ^{234}U(γ,f) and ^{232}Th(γ,f) reactions and investigated the possibility of relating the mass and angular distribution correlations to the two standard modes of fission (Brosa et al., 1990).

2. Experimental setup and procedure

The experiments were performed at the Darmstadt High-Intensity Photon Setup (Mohr et al., 1999; Sonnabend et al., 2011), located at the end of the superconducting injector linac of the Superconducting Darmstadt linear accelerator (S-DALINAC (Richter, 1996)). The S-DALINAC electron beam was used to produce bremsstrahlung in a radiator consisting of four copper sheets. After passing a copper collimator the bremsstrahlung reached the fission target placed inside the fission fragment detector, a twin Frisch-grid ionization chamber. The fission targets consisted of thin layers (<90 μg/cm^2) of UF_4 or ThF_4 vacuum-evaporated onto one side of thin (∼35 μg/cm^2) polyimide foils with thin gold layers (∼50 μg/cm^2) evaporated onto the opposite side. The twin Frisch-grid ionization chamber consists of two ionization chambers placed back-to-back on a common cathode. The fission target is placed in a hole in the common cathode, allowing coincident detection of the two fission fragments. The cathode–grid distance was 3 cm, while the grid-anode distance was 0.5 cm. The volume between the electrodes is filled with P-10 gas (90 % Ar + 10 % CH_4) at a pressure of 1.05 bar, continuously flowing through the chamber at a flow rate of about 60 ml/min. The Frisch-grids were kept at ground potential, the operating voltage for the cathode (-1.6 kV) was chosen in order to ensure stability of the pulse-height defect (Tovesson et al., 2002) and drift velocity (Kryachkov et al., 2003), for small variations in reduced field strength. The operating voltages for the anodes (+1.0 kV) were chosen to avoid collection of electrons on the grid (Bunemann et al., 1949).

2.1. Data analysis

The determination of fission fragment masses is based on the well established double kinetic energy (2E) technique. Conservation of linear momentum, with the approximation that the mass of the two fission fragments is equal to the mass of the fissioning nucleus leads to the following relation

$$A_{1,2} = A_f \frac{E_{2,1}}{\mathrm{TKE}}, \tag{1}$$

where $A_{1,2}$ and $E_{1,2}$ are the fragments' mass numbers and kinetic energies, respectively, TKE = $E_1 + E_2$ is the total kinetic energy, and A_f is the mass number of the fissioning nucleus. The emission angle was extracted from the drift time of ionization electrons, which, besides the determination of angular distributions, allowed correction for angle dependent systematic errors in the pulse height data. A detailed description of the procedure for determining the emission angles and the subsequent corrections to the pulse height data can be found in Ref. (Göök et al., 2010). The pulse-height defect (PHD) of the counting gas was taken into account in calibrating the measurement using results on bremsstrahlung induced fission of ^{238}U at E_0 = 8.5 MeV from Pommé et al. (1994), with a parameterization of the PHD according to Budtz-Jørgensen et al. (1987). Prompt neutron evaporation by the fission fragments was taken into account using experimental data from Apalin et al. (1965) and Piessens et al. (1993).

3. Experimental results and discussion

Pre-neutron fission fragment mass distributions for ^{238}U, ^{234}U and ^{232}Th are displayed in Fig. 1. The mass yield is normalized to 200 %. The distributions have been labeled with the calculated average excitation energies and consecutively displaced by 2 %. The preference for an asymmetric mass split, characteristic for low-energy fission of actinide nuclei, is easily recognized in all the mass distributions. The results for ^{238}U(γ,f) agree well with earlier experiments (Pommé et al., 1994). For ^{234}U the mass yield in the region above $A_H \sim 140$ increases going from $\langle E_x \rangle$ = 7.23 MeV to $\langle E_x \rangle$ = 6.49 MeV, while the mean heavy-fragment mass remains constant within the statistical uncertainty. Further lowering of the excitation energy causes a decrease in mass yield above $A_H \sim 140$, which leads to a slight decrease in the mean heavy-fragment mass. For ^{232}Th an increase in the mass region above $A_H \sim 140$ is observed, going from $\langle E_x \rangle$ = 7.26 MeV to $\langle E_x \rangle$ = 6.68 MeV.

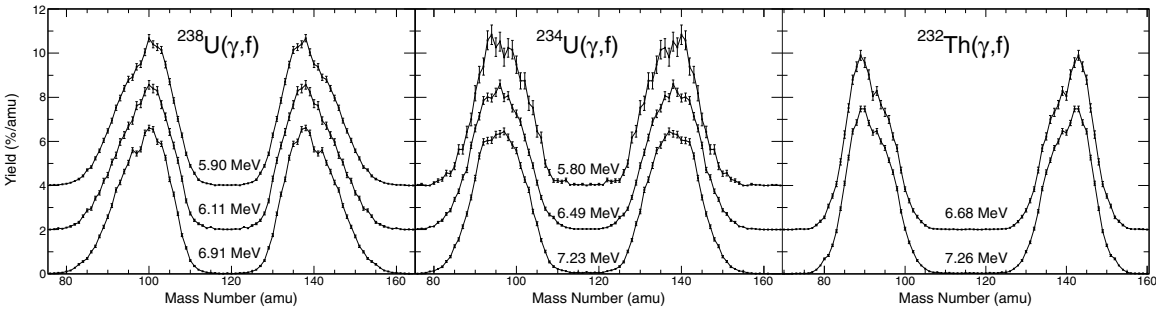

Fig. 1. Fission-fragment yield as a function of fission-fragment mass number from the reactions ^{238}U(γ, f), ^{234}U(γ, f) and ^{232}Th(γ, f). The curves are consecutively displaced by 2% and labeled with the average excitation energy.

3.1. Identification of fission modes

Further investigation of the experimental data was performed within the multi-modal random-neck-rupure model (Brosa et al., 1990). Three fission modes were considered; the two mass-asymmetric standard modes (S1, S2) and the mass-symmetric superlong mode (SL). The contribution of a particular fission mode to the yield as function of mass and total kinetic energy is described by

$$Y(A,\mathrm{TKE}) = \frac{w}{\sqrt{2\pi\sigma_A}} \exp\left(-\frac{(A-\langle A\rangle)^2}{2\sigma_A^2}\right) \times \left(\frac{200}{\mathrm{TKE}}\right)^2 \exp\left(\frac{-(L-l_{max})^2}{(L-l_{min})\,l_{dec}}\right), \tag{2}$$

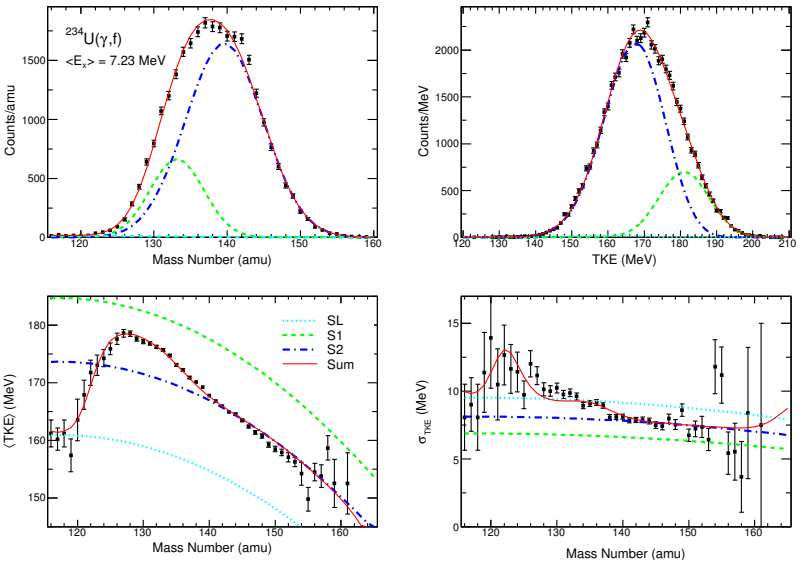

Fig. 2. Fission-fragment yield as a function of mass (top left) and TKE (top right) as well as average TKE (bottom left) and width (bottom right) as function of the fragment mass from ^{234}U(γ, f) at $\langle E_x\rangle$ = 7.23 MeV. The solid red lines represent results from fits according to Eq. (2), the different colored lines are the model components.

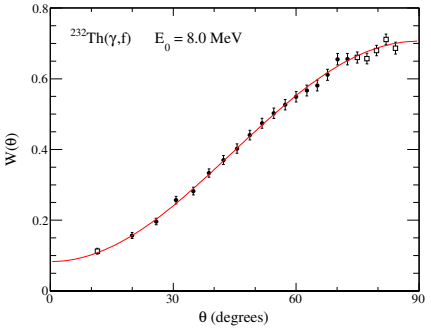

Fig. 3. Fission-fragment angular distribution from ^{232}Th(γ, f) at bremsstrahlung endpoint energy E_0 = 8.0 MeV. The solid line shows the best fit of Eq. (4) to the region indicated by the full black circles.

where L is the distance between the charge centers of the fragments at scission. Considering only the Coulomb interaction this quantity may be approximated by

$$L = \frac{Z_L Z_H e^2}{\mathrm{TKE}} \approx \frac{A_L A_H (\frac{Z_F}{A_F})^2 e^2}{\mathrm{TKE}}. \tag{3}$$

The parameters of Eq. (2) have the following intuitive meanings:

- The most probable distance between the fragment charge centers at scission is denoted by l_{max},
- the smallest allowed distance by l_{min}.
- The exponential decrease in yield with simultaneous increase in L is described by l_{dec},
- and w represents the weight of the mode.

The fits described the measured distributions well for all sets of data, details can be found in Ref. (Göök, 2012). An example of the fit is shown in Fig. 2, displaying data from ^{234}U(γ,f) at $\langle E_x \rangle$ = 7.23 MeV together with the results of the fits. The characteristic parameters of the mass distribution obtained from the fits to the ^{238}U data are in agreement with theory (Brosa et al., 1990) as well as earlier experimental investigations (Pommé, 1992). We note that for the ^{234}U(γ,f) reaction we deduced mode weights different from a preceding study (Göök et al., 2011). This discrepancy can be shown to arise from an increased target thickness used in the previous experiment (Göök, 2012).

3.2. Angular distributions

The experimentally found fission-fragment angular distributions are parameterized by the theoretically expected ones, given by the expression

$$W(\theta) = A + B \sin^2 \theta + C \sin^2 2\theta, \tag{4}$$

which is normalized according to $\int_0^\pi W(\theta) \sin\theta d\theta = 1$. Angles close to 90° are excluded from the fit, since there the data is influenced by absorption and scattering in the target. Angles close to 0° are excluded as well, due to the uncertainty introduced by the limited angular resolution. In Fig. 3 the angular distribution determined for ^{232}Th(γ, f) at bremsstrahlung endpoint energy E_0 = 8.0 MeV is shown as an example. The experimental data is obviously well described by the fit to Eq. (4), represented by the solid red line. As expected for the photofission of ^{232}Th, the angular distribution shows a distinct dipole pattern, peaked at θ = 90°. The first hint for a correlation between the fission-fragment masses and their angular distribution can be seen in Fig. 4, which shows the distinctly different angular distribution patterns found for a quasi-symmetric (S) and an asymmetric (A) mass cut. The mass cuts shown on the right-hand side of Fig. 4 were rather arbitrarily chosen, and a more quantitative procedure is desirable. This is achieved by the introduction of a parameter M^*, according to

$$W(\theta, M^*) = \int_{A=M^*}^{\infty} W(\theta, A) dA, \tag{5}$$

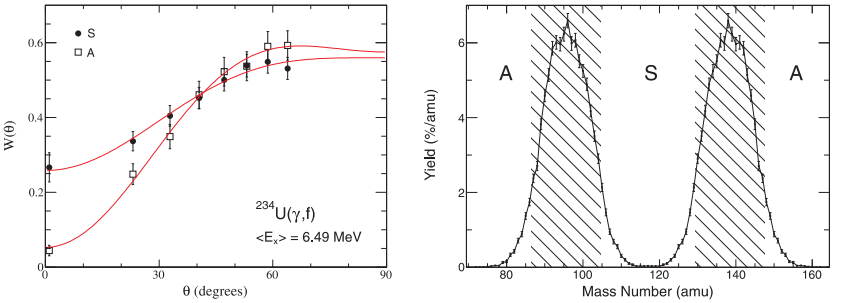

Fig. 4. Angular distribution from ^{234}U(γ,f) at E_0 = 7.5 MeV in a quasi-symmetric (S) and an asymmetric (A) mass region, as indicated on the right hand side. Only events with $\cos\theta \geq 0.4$ are shown, since the mass cuts are not defined for lower values of $\cos\theta$

where A is the heavy-fragment mass number. Similarly, for the TKE dependence a parameter TKE* is introduced, according to

$$W(\theta, \mathrm{TKE}^*) = \int_{\mathrm{TKE}=\mathrm{TKE}^*}^{\infty} W(\theta, \mathrm{TKE}) d(\mathrm{TKE}). \tag{6}$$

For each value of the parameters M^* and TKE* the expression in Eq. (4) is fitted to the resulting angular distribution. The result of applying this procedure on the ^{232}Th(γ, f) data at E_0 = 9.5 MeV, and the ^{234}U(γ, f) data at E_0 = 9.0 MeV is shown in Fig. 5. An increase in the anisotropy B/A correlated with an increase in M^* is seen for both ^{232}Th and ^{234}U, similarly an increase in the parameter TKE* is correlated with a decrease in the anisotropy B/A. This gives a consistent picture when keeping the $\langle \mathrm{TKE} \rangle(A)$ dependence in mind. For the asymmetric mass peak, the further away from symmetric mass splits, the lower is the TKE, neglecting the low yield symmetric component.

Assuming that each fission mode has a fixed set of angular distribution coefficients for a particular bremsstrahlung endpoint energy, as suggested by Knitter (1991), the fission mode yield can be used to calculate the dependence of the angular distributions on mass and TKE. The mode-specific angular distribution coefficients can then be extracted from a fit to the data displayed in Fig. 5. If different outer barriers of the standard modes are responsible for the mass and TKE dependence of the angular distributions, the same set of parameters must describe both dependences simultaneously. The red lines in Fig. 5 display the result of a fit to the TKE dependence, here the same set of parameters also describes qualitatively the mass dependence. Similar mass and TKE dependences of angular distributions were found for all investigated bremsstrahlung endpoint energies, and the same procedure for extracting mode-specific angular distribution coefficients could be applied. The result for the ratio B/A sensitive to the outer barrier is shown in Fig. 6, as function of the bremsstrahlung endpoint energy. It was found that the B/A ratio for the S2 mode is larger than for the S1 for all endpoint energies in both ^{232}Th and ^{234}U. The fact that the mass and TKE energy dependence of the outer barrier sensitive B/A ratio of angular distributions exist and can be described by the standard modes of fission is a strong indication that separate outer barriers do exist for the standard modes, as suggested on theoretical grounds in Oberstedt et al. (1998); Duijvestijn et al. (2001); Vladuca et al. (2002). With more excitation energy available on top of the barrier, a smaller value for the B/A-ratio is expected (Jacobs and Kneissl, 1991). The result that the B/A-ratio for the S2 mode is larger than for the S1 mode suggests that the outer barrier for the S2 mode has a lower penetrability. This is contrary to what is expected from the relative yield of the standard modes, hence the relative importance of the standard modes cannot be exclusively a consequence of different outer barrier penetrabilities. In order to understand this contradiction it will be interesting to extend the experiments to lower excitation energies, with the aim of extracting quantitative information on barrier heights and curvatures from mode separated angular distributions.

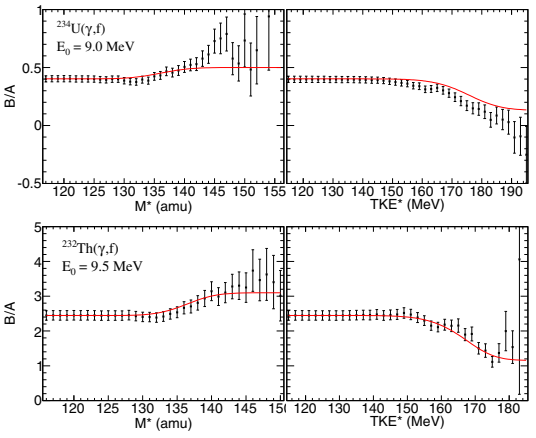

Fig. 5. Dependence of the ratio B/A of angular distribution coefficients on mass and TKE cut off parameters in ^{234}U at E_0 = 9.0 MeV (top) and ^{232}Th at E_0 = 9.5 MeV (bottom). Data on mass and TKE cuts according to Eqs. (5) and (6) are shown as points. The solid red curve indicates the calculated behavior based on independent angular distributions for the two standard fission modes.

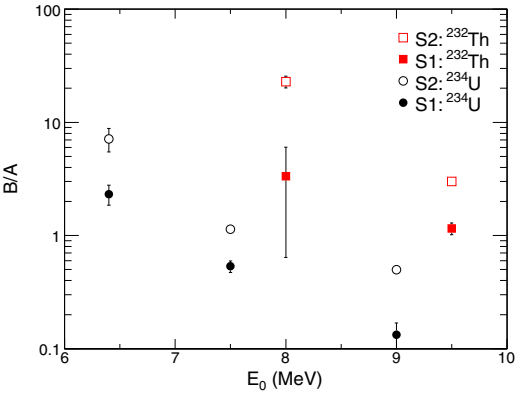

Fig. 6. Ratio B/A of the angular distribution coefficients determined for the two standard fission modes in ^{234}U(γ,f) and ^{232}Th(γ,f) as function of the bremsstrahlung endpoint energy.

Acknowledgements

This work was supported by the Deutsche Forschungsgemeinschaft through SFB 634 and by the State of Hesse through the Helmholtz International Center for FAIR within the LOEWE initiative.

References

Apalin, V., Gritsyuk, Y. N., Kutikov, I., Lebedev, V., Mikaelian, L., 1965. Nucl. Phys. 71, 533.
Bohr, A., 1956. in Proc. Int. Conf. Peaceful uses of Atomic Energy I, 151.
Brosa, U., Grossmann, S., Müller, A., 1990. Phys. Rep. 197, 167.
Budtz-Jørgensen, C., Knitter, H.-H., Straede, C., Hambsch, F.-J., Vogt, R., 1987. Nucl. Instr. and Meth. A 258, 209.
Bunemann, O., Cranshaw, T., Harvey, J., 1949. Can. Jour. Res. A 27, 191.
Duijvestijn, M. C., Koning, A. J., Hambsch, F.-J., 2001. Phys. Rev. C 65, 014607.
Göök, A., 2012. Dissertation D17. url http://tuprints.ulb.tu-darmstadt.de/3166/, Technische Universität Darmstadt.
Göök, A., Chernykh, M., Eckardt, C., Enders, J., von Neumann-Cosel, P., Oberstedt, A., Oberstedt, S., Richter, A., 2011. Nucl. Phys. A 851, 1.
Göök, A., Chernykh, M., Enders, J., Oberstedt, A., Oberstedt, S., 2010. Nucl. Instr. and Meth. A 621, 401.
Jacobs, E., Kneissl, U., 1991. in: The nuclear fission process. Ed. C. Wagemans, CRC Press, Boca Raton, Florida, Ch. 5, p. 103.
Knitter, H.-H., 1991. in: The nuclear fission process. Ed. C. Wagemans, CRC Press, Boca Raton, Florida, Ch. 10, p. 491.
Kryachkov, V., Dunaeva, I., Dunaev, M., Semenova, N., Seergachev, A., 2003. Instruments and Experimental Techniques 46, 804–813.
Mohr, P., Enders, J., Hartmann, T., Kaiser, H., Schiesser, D., Schmitt, S., Volz, S., Wissel, F., Zilges, A., 1999. Nucl. Instr. and Meth. A 423, 480.
Oberstedt, S., Hambsch, F.-J., Vivés, F., 1998. Nucl. Phys. A 644, 289.
Piessens, M., Jacobs, E., Pommé, S., De Frenne, D., 1993. Nucl. Phys. A556, 88.
Pommé, S., 1992. Dissertation, Universiteit Gent.
Pommé, S., Jacobs, E., Piessens, M., De Frenne, D., Persyn, K., Govaert, K., Yoneama, M.-L., 1994. Nucl. Phys. A 572, 237.
Richter, A., 1996. In: Proc. Fifth European Particle Accelerator Conference, Sitges/Spain 1996. Institute of Physics Publishing, Bristol, Philadelphia, p. 110.
Sonnabend, K., Savran, D., Beller, J., Büssing, M., Constantinescu, A., Elvers, M., Endres, J., Fritzsche, M., Glorius, J., Hasper, J., Isaak, J., Löher, B., Müller, S., Pietralla, N., Romig, C., Sauerwein, A., Schnorrenberger, L., Wälzlein, C., Zilges, A., Zweidinger, M., 2011. Nucl. Instr. and Meth. A 640, 6.
Steiper, F., Frommhold, T., Henkel, W., Jung, A., Kneissl, U., Stock, R., 1993. Nucl. Phys. A 563, 282.
Tovesson, F., Hambsch, F.-J., Oberstedt, S., Bax, H., 2002. Nucl. Scien. Tech. Suppl. 2, 673.
Vladuca, G., Tudora, A., Hambsch, F.-J., Oberstedt, S., 2002. Nucl. Phys. A 707, 32.
Wilke, W., Heil, R., Kneissl, U., Seemann, U., Steiper, F., Ströher, H., Weber, T., 1988. Phys. Lett. B 207, 385.